Experimental study of NO_x reduction on a Medium Speed Heavy Duty Diesel engine by the application of EGR and Miller timing

Roel Verschaeren[a], Wouter Schaepdryver[a], Thomas Serruys[a], Marc Bastiaen[b], Lieven Vervaeke[b], Sebastian Verhelst[a]

[a] *Ghent University*
[b] *Anglo Belgian Corporation NV*

Abstract

Emission legislation that applies to engines used in shipping, rail and land power generation becomes increasingly strict. E.g. IMO Tier III applicable to sea-going vessels limits the NO_x emission by 75% compared to IMO Tier II. Attaining these without sacrificing fuel consumption is a big challenge. This paper reports on engine internal measures that can provide a viable alternative to expensive (running costs) and bulky after-treatment. Exhaust Gas Recirculation (EGR) and early intake valve closing as NO_x reduction techniques are mature technologies on automotive applications but on medium speed diesel engine as investigated here, these are still not straightforward to implement. Two camshaft configurations are considered under EGR operation. In this research, a new approach for determining the EGR rate is developed. The effects of various EGR rates on fuel consumption and engine-out emissions are investigated, while in-cylinder pressure measurements and calculated apparent heat release rates (AHRR) provide more insight into the physical effects of EGR on the combustion.

Keywords: medium speed, diesel, heavy duty engine, EGR, Miller timing, NO_x

1. Introduction

The diesel engine has been the main power source in freight transport (road, rail and water) and various Heavy Duty (HD, here considered as shipping, rail and land power generation) for decades. This will not change in the coming years, owing to its main assets: high efficiency under part and full load and high durability. However, the diesel engine suffers from high NO_x and PM emissions due to its non-premixed combustion operation and the short available mixing time in the combustion chamber.

In recent years the legislative organizations such as IMO, EPA and EU have implemented progressively more stringent emission limits. For example IMO Tier III requires the emission of NO_x to be reduced by more than 75% compared to IMO Tier II. This forces engine manufacturers to use more advanced measures for emission reduction while trying to preserve high efficiencies. Some techniques, mainly proven in the automotive field are reconsidered and evaluated for their emission reduction potential.

After-treatment solutions allow for very strong reductions in harmful emissions [1] but require additional space, which is a clear disadvantage in rail, water and road transport. Furthermore after-treatment has a high capital-, and operational cost (e.g. Diesel Exhaust Fluid or DEF). To avoid these disadvantages in-cylinder measures can provide a worthy alternative.

One option is the use of EGR, a technique commonly used in automotive diesel engines for its high NO_x reducing potential, which starts to find entry in high-power medium speed diesel engines [2].

Advancing Inlet Valve Closure (IVC) or Miller timing is another technique used to lower NO_x. Closing the intake valve early shortens the effective intake and compression strokes compared to the expansion and exhaust strokes. This provides internal cooling and a lower temperature at the end of compression is achieved, which results in lower NO_x emissions [3]. In [4] a 2.8l 4 cylinder automotive diesel engine was studied and Inlet Valve Closure was varied between 492°CA and 540°CA and compared to the baseline. The most important NO_x

decrease was found at high load without a large penalty on fuel consumption. Using the European Driving Cycle they found a 25% decrease in NO_x emission using optimized Miller timing.

A relatively small heavy duty diesel engine (a 1.8l single cylinder engine, representing truck engines) was investigated in [5, 6]. It was found that the combined application of EGR and advanced IVC caused an important reduction in NO_x emissions, while the engine efficiency reduced slightly because of a lower effective compression ratio.

In [7] the combination of EGR and Miller timing was investigated using a simulation tool for a low speed ($1000rpm$) heavy duty diesel engine ($200kW/cylinder$). The intake pressure was increased to recover the original intake mass flow rate. From the simulations, it was found that significant NO_x reductions (-35%) could be achieved while maintaining fuel consumption. When allowing a 3% increase in fuel consumption the NO_x emission could be decreased by 90%, according to the simulation.

Very high injection pressures, combined with multiple injections every cycle are now commonly used in high speed direct injected diesel engines [8]. High injection pressures atomize the spray into very fine droplets, which allows for easier evaporation and decreasing smoke, HC and CO emissions. Using multiple injections in every cycle, the heat release rate can be shaped to prevent high temperatures and NO_x formation.

The main objective of this investigation is to validate and quantify the effect of early IVC and EGR on a medium speed high power diesel engine. The considered engine is a multi-cylinder engine, it has a $256mm$ bore and high power ($220kW/cylinder$) whereas previous work is limited to automotive and truck applications and corresponding lower power output. In this work the influence of EGR and camshaft configuration on fuel consumption and the main pollutant emissions, NO_x, UHC and CO is investigated. In-cylinder pressure measurements provide insight into the physical effects of EGR on the combustion by calculating AHRR and MFB.

2. Experimental setup

2.1. Six-cylinder medium speed diesel engine

A modified version of an Anglo Belgian Corporation (ABC) six-cylinder medium speed diesel engine is used for testing. The most important specifications are listed in Table 1. Two configurations are compared, a configuration using standard valve timing and one using (moderate) Miller timing. The engine is equipped with a fixed geometry turbocharger. Because the engine is built with durability and reliability in mind, it is not easy to change injection timing, nozzles, injection pressure or valve timing. Almost every parameter is mechanically fixed, which means that changing an operating parameter requires partial disassembly of the engine and a considerable amount of time. The engine can currently be certified for operation under IMO II ($NO_x < 8.98 g/kWh$, no visible smoke) and inland waterway EUIIIa (combined $NO_x + HC < 8.7 g/kWh$) regulations.

Cylinder configuration	6 in line
Bore [mm]	256
Stroke [mm]	310
Rated power [kW]	1326
Rated speed [rpm]	1000
Compression ratio	14:1
Injection system	pump-line-nozzle
SOI [°BTDC]	21
Miller IVC [°BBDC]	20
Standard IVC [°BBDC]	-40
EVO [°ATDC]	118

Table 1: ABC test engine specifications

Figure 1 shows an overview of the EGR setup, which in contrast to all the other operating parameters is designed to be very flexible. A high-pressure

cooled EGR loop is used. Exhaust gas is extracted upstream of the main turbine, sent through a water-cooled heat exchanger and redirected into the inlet manifold. The pressure downstream of the air compressor is higher than the exhaust gas extraction pressure, preventing natural flow through a valve from exhaust to inlet manifold. Therefore a small turbo compressor, commonly referred to as 'EGR pump', is used to overcome this pressure difference.

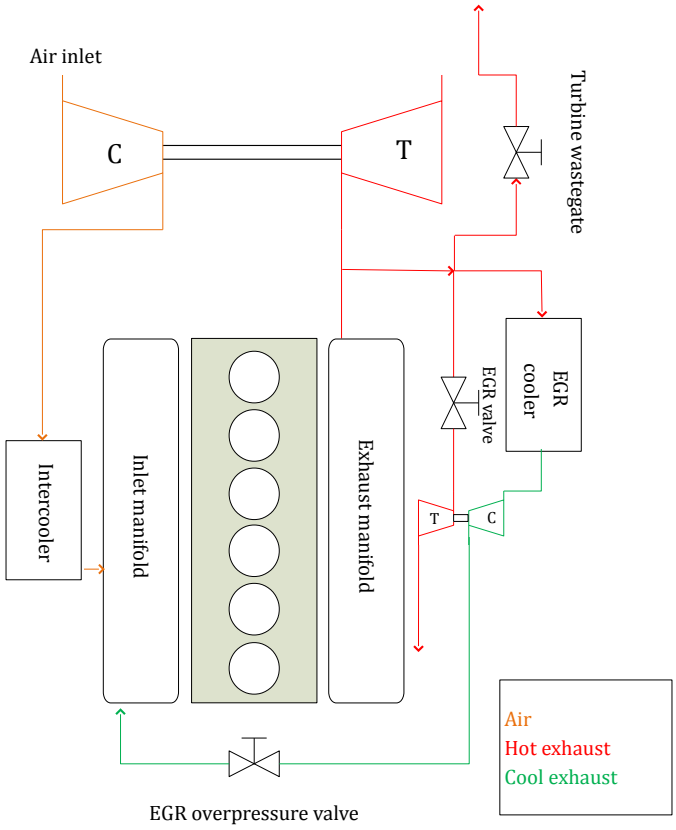

Figure 1: EGR setup

The main turbocharger is optimized to give adequate boost pressures when using EGR and a Miller camshaft. Under EGR operation, a portion of the exhaust gas stream is diverted before entering the main turbine, thereby lowering turbine flow. As a result, a turbine wastegate is required for operation without EGR at high loads to prevent combustion pressures from exceeding the

engine limit. The main turbine has a maximum inlet temperature of 650 °C, specified by the manufacturer. Together the pressure and temperature limit set the boundaries for the operational window during high load tests. It is important to note that this EGR setup lowers the inlet manifold pressure (IMP) with increasing EGR rate.

2.2. Measurement procedure

The setup at ABC allows the measurement of power through evaluation of the electric power delivered by a generator, driven by the engine. Fuel consumption is acquired through a digital weighting scale during a certain amount of time. The individual emission components are measured using a *Sick GMS810* gas analyzer, giving dry NO_x, CO, CO_2 and O_2 and wet UHC concentrations. Measurement errors from this equipment is given in Table 2. The emission values in [ppm] or [vol%] are converted to specific values in [g/kWh] through procedures outlined in [9]. Unless stated otherwise, all reported emission values in the next sections are specific emissions.

	Relative Error [-]	**Absolute Error**
m_{fuel} [kg]	/	0.05
t_{fuel} [s]	/	0.1
CO_2 [vol%]	0.05	/
O_2 [vol%]	0.029	/
NO_x [ppm]	/	12
CO [ppm]	/	10
HC [ppm]	/	14
PM [mg/Nm^3]	/	4

Table 2: Accuracy emission measurement

For the in-cylinder pressure measurements an *AVL QC34D* piezoelectric relative pressure transducer was installed in cylinder 6. Absolute pressure transducers (*Kistler 4075A10*) were mounted in the inlet and exhaust manifolds. A

National Instruments cDAQ 9174 data acquisition system was used to record 200 cycles at every test point. Each full crankshaft rotation delivers 500 sample pulses through a *Heidenhain ROD430* crank angle encoder, resulting in a system with a resolution of 0.72°CA.

The load points were chosen based on the operating points specified in the emission test cycle. In the IMO III emission cycles, the 75% and 100% load points have the highest weighting factors, 0.5 and 0.2. For this reason the focus of this paper lies on these points. The engine is rated $1326kW$ at $1000rpm$: the 100% load point. By using the propeller law [10] the 75% load point corresponds to $910rpm$.

3. Methodology

3.1. Cylinder pressure pegging

The relative in-cylinder pressures can be converted to absolute pressures in different ways. Three pegging options were evaluated:

- pegging to IMP around BDC
- pegging to Exhaust Manifold Pressure (EMP) around TDC
- pegging during compression stroke using the polytropic index

Due to the application of a Miller camshaft, pegging to IMP was discarded. It cannot be guaranteed that the cylinder charge pressure is equal to the measured IMP when the intake valve closes before BDC due to pressure losses over the intake valve. Pegging to EMP was discarded due to the relatively large pressure fluctuations of the in-cylinder pressure trace around exhaust valve closure (EVC). These fluctuations can be traced back to valve action close to the transducer. As a result, a compression pegging method was chosen for pressure referencing.

In internal combustion engines, the process in the early compression stroke can be described as a polytropic process. The absolute pressure-volume relation

is given by

$$log(p_{abs}) = \gamma \cdot log(V) \tag{1}$$

An iterative pegging algorithm was applied to the pressure traces during the compression stroke, as described in [11]. Two outer bounds for the pressure shift are chosen, Δp_{max} and Δp_{min} . The mean of these shifts is chosen as a first pressure offset approximation Δp, which is applied to the pressure data early in the compression stroke. This approximation is fitted to a 2d-order polynomial regression

$$log(p_{rel} + \Delta p) = C_1 \cdot log(V)^2 + C_2 \cdot log(V) + C_3 \tag{2}$$

The sign of C_1 determines whether Δp is to be used in the next iteration as the new Δp_{max} or Δp_{min} in the next iteration. The use of equation 2 is repeated until C_1 approaches zero. For the corresponding Δp, the pegged in-cylinder process in the early compression stroke closely fits the linear relationship in equation 1.

The pegging algorithm avoids having to use a fixed, thus estimated polytropic index for all test points, as has been used in previous work at ABC [12].

3.2. Measuring EGR rate

In order to correctly assess the influence of EGR on engine performance, an accurate determination of EGR% is needed. EGR% is defined as

$$EGR\% = \frac{\dot{m}_{EGR}}{\dot{m}_{EGR} + \dot{m}_{air}} \cdot 100 \ [\%] \tag{3}$$

In the past, two techniques were used to calculate EGR%: the [O_2]-method and the DMAF-method (Differential Mass Air Flow) [12, 13]. The [O_2]-method was inaccurate presumably because of bad mixing at the measuring location in the inlet manifold. This caused a high variability between the measurements. For every operating point the DMAF method required a reference measurement without EGR at the same inlet manifold pressure and temperature as the considered EGR test point. With some assumptions, the EGR rate was

then determined with airflow measurements in the inlet. This method was very sensitive on the reference measurement and was very time-consuming.

Therefore, an energy balance method was developed, using the energy transfer in the EGR cooler from the recirculated gases to the cooling water. The energy balance states

$$\dot{m}_{EGR} = \frac{\dot{m}_{water} \cdot c_{p,water} \cdot \Delta T_{water} - \dot{m}_{cond} \cdot L}{c_{p,EGR} \cdot \Delta T_{EGR}} \, [\frac{kg}{s}] \tag{4}$$

where the second term $\dot{m}_{cond} \cdot L$ is added to account for condensation of water vapor from the exhaust gas.

On the water side mass flow and temperatures are measured and on the gas side, pyrometers and thermometers are used to measure the inlet and exhaust temperatures. Water heat capacity is taken as $c_{p,water} = 4.186 \; kJ/kgK$. The measured variables in 4 have a relatively low variability yielding consistent results. This might not be expected but in this application the mass flow rate from the exhaust gas in the EGR-cooler is high compared to an automotive application, which together with a high ΔT_{EGR} ($> 200K \pm 5K$) and ΔT_{water} ($> 15K \pm 1K$) results in accurate EGR%. The heat exchange in the cooler at maximum EGR% is $298kW$. The combined relative error on EGR% is 2.15%.

The energy balance EGR% method has been compared to the previously used methods in Figure 2. The case of 100% load at 1000 rpm is considered for varying EGR%. NO_x-emissions have been normalized relative to the emission value without EGR.

The $[O_2]$-method results in unrealistically high NO_x reductions for small EGR% and has large measurement uncertainties for low EGR%. Since the $[O_2]$ is measured in the intake manifold, a possible explanation is insufficient mixing between the intake air and the recirculated exhaust gas at the $[O_2]$ measurement location. The DMAF method provides more realistic results but suffers from high uncertainties throughout the entire range, and the necessity of reference test points for each measurement.

The cooler method has much smaller uncertainty intervals and produces a quasi-linear trend: decreasing NO_x with increasing EGR%. This general trend

has been documented in multiple studies [14]. Other advantages include the use of inexpensive measuring equipment, low maintenance (no fouling of gas concentration probes) and the absence of reference measurements. The energy balance method is chosen as the preferred method for calculating the EGR% in this paper.

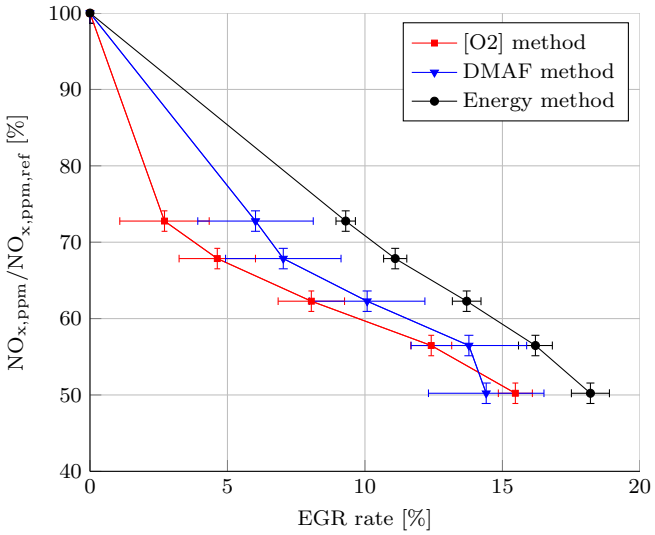

Figure 2: Comparison of EGR% methods, 100 % load, 1000 rpm

3.3. Heat Release Rate

In-cylinder pressure data can be used to assess the effect of EGR on the apparent heat release rate (AHRR), cumulative heat release (HR) and mass fraction burned (MFB) in the combustion process. AHRR is defined as [15]:

$$AHRR(\theta) = \frac{\gamma}{\gamma - 1} \cdot P_{cyl}(\theta) \cdot \frac{dV(\theta)}{d\theta} + \frac{1}{\gamma - 1} \cdot V(\theta) \cdot \frac{dP_{cyl}(\theta)}{d\theta} \; [\frac{J}{^\circ CA}] \tag{5}$$

In equation 5 $\gamma = 1.34$ is used, as advised in literature. HR is obtained by integration of the AHRR between IVC and EVO. MFB was calculated as the fraction of released heat between the minimum HR after SOI and maximum HR

before EVO.

$$MFB(\theta) = \frac{HR(\theta) - HR_{min}}{HR_{max} - HR_{min}} \ [-] \tag{6}$$

These two limits of HR mark the start and end of combustion. The definition relative to the minimum HR is necessary to account for the fuel evaporation effect on HR.

4. Results

4.1. Effects of EGR on the combustion process

The recirculation of exhaust gases into the cylinder significantly changes the combustion process. The well-known effects of EGR include thermal effects, dilution effects and chemical effects [14, 16]. Figure 3 shows the influence of EGR on AHRR for a series of tests at 75% load, 910 rpm. As mentioned earlier, it has to be taken into account that in this setup, an increase in EGR is accompanied by a decrease in inlet manifold pressure as part of the exhaust flow is diverted from the main exhaust turbine, lowering compression pressure and IMP. This should be kept in mind when explaining observed trends, since the two variables EGR and IMP are always changing simultaneously.

With increasing EGR% in the setup, an increase in ignition delay is observed which is especially clear when using Miller timing. This can be explained by the thermal effect of EGR. The larger heat capacity of the in-cylinder mixture (due to larger amounts of CO_2 and H_2O) under EGR operation lowers temperatures during compression, delaying the onset of ignition. The cooling due to the Miller timing has a large influence as can be seen from the standard valve timing, where this cooling is not present and ignition delay is almost unchanged. Also, the EGR dilution effect plays a role. The decreasing $[O_2]$ in the mixture increases ignition delay [17]. A final influence on the longer ignition delay is the accompanying lower IMP under EGR operation. The lower intake mass flow also results in lower compression pressures and temperatures. This was reported in previous research at ABC [12].

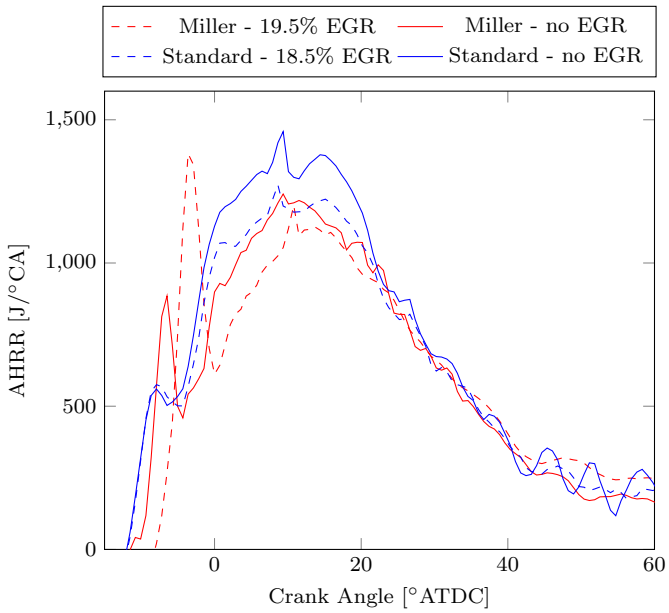

Figure 3: AHRR for changing EGR% and changing IVC at 75% load, 910 rpm

The height of the premixed peak is governed by two opposing effects [18]. Firstly, the lower global O_2-concentration would suggest a decrease in premixed combustion. On the other hand, the longer ignition delay provides a longer mixing time for the injected fuel before ignition. Thus a larger amount of fuel can be burned in the premixed phase. From Figure 3 it is clear that the latter effect is dominant in this setup, resulting in a higher premixed AHRR peak with increasing EGR%.

The majority of the fuel is burned in the second combustion stage, the diffusion combustion. The intensity of the diffusion combustion just after TDC is lowered with increasing EGR%. The same thing happens when using Miller valve timing, it lowers the intensity of the diffusion combustion in comparison to standard valve timing. This gives rise to lower temperatures in the first part of the diffusion combustion. The higher heat capacity of the mixture under EGR operation also lowers the temperature. Further down the stroke, the AHRR drops slower when increasing the EGR%. A larger part of fuel is combusted

further away from TDC. The calculated MFB angles for Miller timing and various EGR% are shown in Figure 4. In this figure the MFB90-line represents the angle where 90% of the fuel is burned. Similar remarks apply to the other lines. Combustion phasing is retarded under EGR and Miller operation and total combustion duration, defined by MFB5-MFB90, is increased. Both effects are expected to have a negative influence on BSFC.

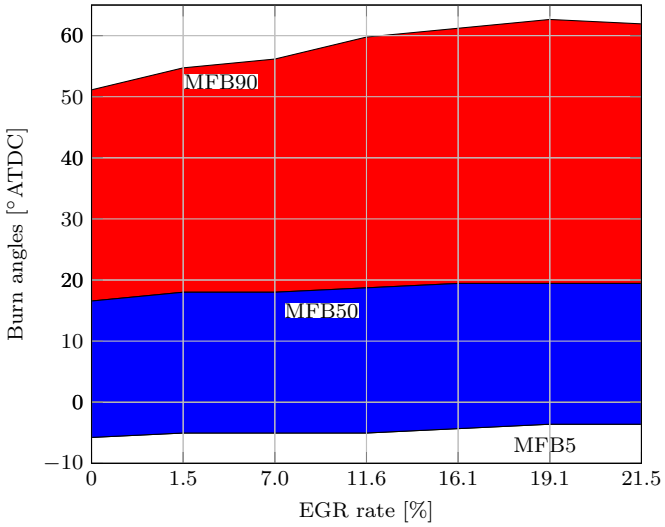

Figure 4: MFB angles at 75% load, 910 rpm, Miller timing

4.2. NO_x emissions

The NO_x emissions for the standard and Miller camshaft configurations are compared at 75% load, 910 rpm in Figure 5. The highest NO_x value (standard valve timing, no EGR) was used as the reference value. To compare the cylinder filling the excess air factor λ is shown on a second axis. λ is calculated according to equation 7 where L_s represents the stoichiometric air-to-fuel ratio. Only fresh air is taken into account in this calculation.

$$\lambda = \frac{\dot{m}_{air,intake}}{\dot{m}_{fuel} \cdot L_s} \; [-] \tag{7}$$

The previously mentioned linearly decreasing trend in NO_x with increasing EGR% is present in both configurations. The maximum EGR% is limited by the main turbine maximum inlet temperature. For the Miller camshaft this results in a maximum of 22% EGR, with the standard camshaft over 25% EGR was reached. This can be explained by the better cylinder filling with the standard camshaft, due to its longer intake time. The better filling is represented by the higher excess air factor. The total amount of mixture in the cylinder has a larger capacity to absorb heat, resulting in lower exhaust temperatures. However, the larger intake mass also results in higher peak pressures. Since the turbocharger has been optimized for use with EGR and Miller camshaft, excessive boost pressures are encountered when operating with the standard camshaft at high load, even when applying EGR. The turbine wastegate has to be used to keep the combustion pressures below the engine limits. The minimum EGR% with standard camshaft without having to use the wastegate is 14%. The break in the excess air factor trend for the 0% EGR point with the standard camshaft, reflects the use of the wastegate.

When comparing each case to its own respective NO_x value without EGR, relative reductions up to 70% are reported for both cases. However, for the Miller camshaft the relative reductions are larger for similar EGR%. Similar maximum NO_x reductions are obtained throughout the entire load range.

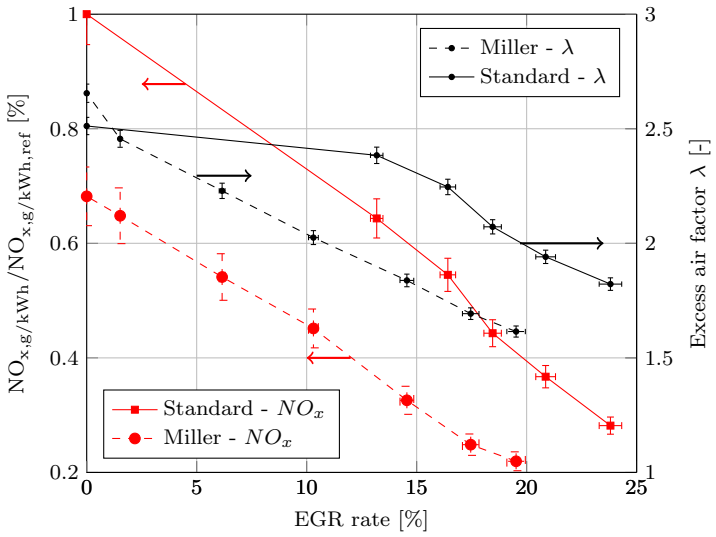

Figure 5: NO_x emissions and air factor at 75% load, 910 rpm

4.3. BSFC/NO_x trade-off

The BSFC for the test points 100% and 75% load is shown in Figure 6. The lowest BSFC value (75% load, Miller timing, no EGR) is used as a reference value. For the 100% load point the wastegate must be enabled when using the standard camshaft, thus biasing the BSFC of the standard operation. When using Miller on 100% load, the wastegate must not be used, this results in a higher efficiency and lower BSFC. The use of the wastegate lowers overall efficiency greatly, since less energy is recovered from the exhaust gases.

From Figure 6 it is clear that the relative BSFC penalty is severe, especially for the Miller configuration. The BSFC increase with EGR% tends to be quadratic. The main cause for the rise in BSFC with increasing EGR% is the effect of EGR on combustion phasing, as discussed earlier.

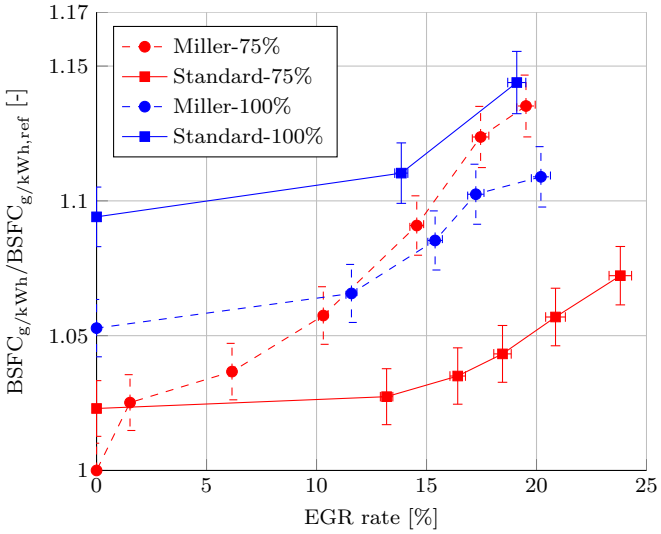

Figure 6: BSFC at 75% load, 910 rpm and 100% load, 1000 rpm

The trade-off between BSFC and NO_x emission for 75% and 100% load is shown in Figures 7 and 8. For the considered test points, the standard camshaft has a more favorable location, as long as the use of the wastegate is avoided. We find that a BSFC penalty of 5% provides a NO_x reduction of more than 50% at the 75% load operating point using Miller timing.

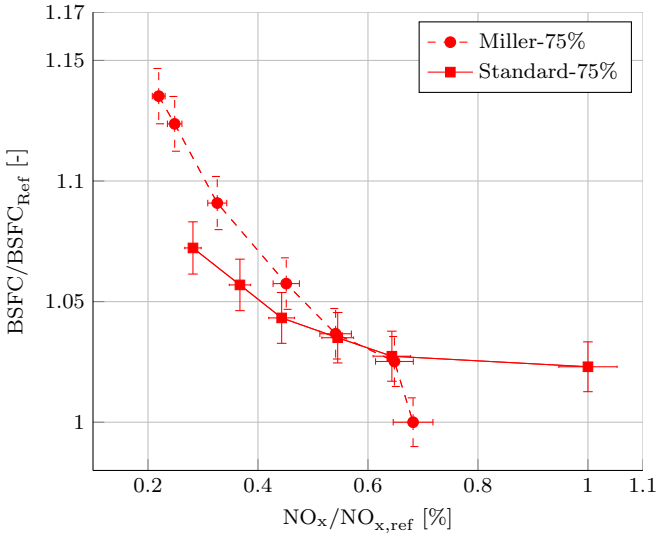

Figure 7: NO$_x$-BSFC tradeoff at 75% load, 910 rpm

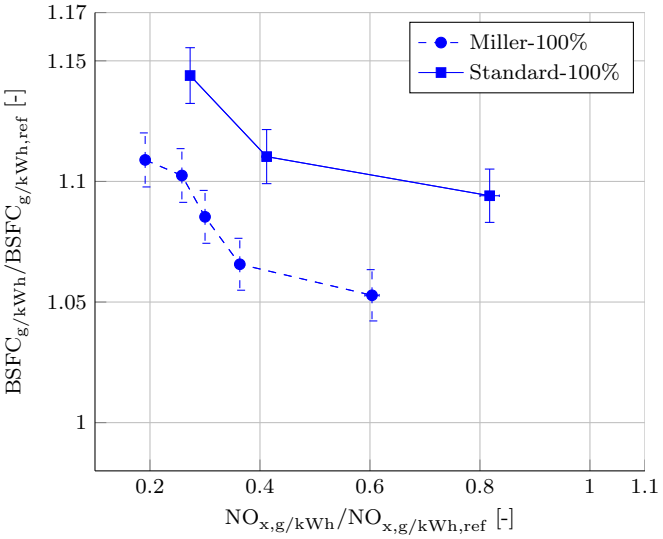

Figure 8: NO$_x$-BSFC tradeoff at 100% load, 1000 rpm

4.4. UHC and CO emissions

The influence of EGR on combustion is also visible in the emission of partial oxidation products. From literature, UHC, CO and PM are expected to increase

due to lower maximum combustion temperatures in the expansion stroke and incomplete combustion. Figure 9 shows the measured specific emissions of CO and UHC as a function of EGR%. A comparison between the Miller and the standard camshaft is made.

Figure 9 shows a strong increase in CO emissions with increasing EGR. When operating with the standard camshaft, CO emission is increasing, mainly due to the temperature and dilution effects of EGR. The rise of CO is much more severe with Miller timing. This can be explained as follows: the lower intake mass with the Miller setup (also visible in Figure 5) and lower compression temperatures (due to the shorter actual compression stroke) result in lower peak pressure and temperature during combustion. Lower peak pressures were observed experimentally, with differences up to 25 bar when compared to standard valve timing and approximately the same EGR%, both for load points 100% and 75%. Lower peak pressures and temperatures prohibit complete oxidation of CO to CO_2. Also, the lower λ under Miller operation and the dilution effect of EGR both lower $[O_2]$, while a high $[O_2]$ is favorable for oxidation of CO.

With the Miller camshaft, UHC emission tends to drop for increasing EGR rate. Specific UHC emission is seen to be relatively constant for standard valve timing. The decrease in UHC emissions is opposed to what is expected from literature.

	no EGR	max EGR
Miller	788 K	923 K
Standard	783 K	813 K

Table 3: Exhaust temperatures 75% load, 910 rpm

The UHC emission behavior in the two setups can be explained by the observed exhaust temperature regimes. Exhaust temperatures with Miller timing are higher than with standard timing, and increase in both setups with increasing EGR%, see Table 3. These observations can be traced back to the combus-

tion phasing: EGR and Miller timing both retard the combustion, increasing combustion further down the expansion stroke, thus increasing the probability for oxidation of HC further down the stroke.

For the standard timing, the change of temperature regimes is not able to significantly alter the combustion of fuel in the late expansion stroke. No clear trend is visible for UHC emissions.

The observed behavior of CO and UHC emission suggests that combustion temperatures, even with EGR, are high enough to ensure the onset of combustion of virtually all fuel droplets, but is inadequate for complete combustion.

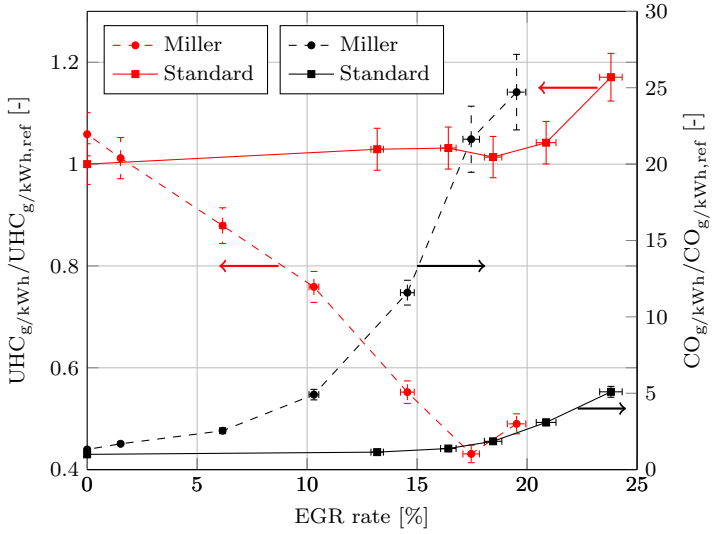

Figure 9: UHC and CO emissions at 75% load, 910 rpm

4.5. PM emissions

Under EGR operation, an increase of PM emissions is expected due to the lower temperatures in the high-temperature part of the combustion. These lower temperatures prevent soot oxidation, resulting in a large net soot emission from the engine. The decrease in $[O_2]$ also impedes soot oxidation.

Generally, it is to be expected that PM increases at lower loads [19]. At lower loads the injection pressures of the mechanical injection system decrease,

lowering atomization and penetration of the fuel, these are necessary to avoid local rich zones.

Figure 10 shows the PM emission at 100% load, 1000 rpm and 75% load, 910 rpm. All measurements use the PM value at 0 EGR%, standard camshaft, as reference.

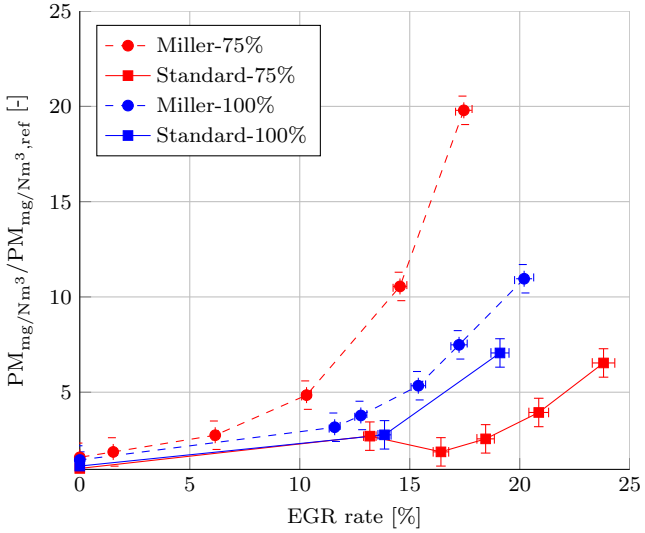

Figure 10: PM emissions at 75% load, 910 rpm and 100% load, 1000 rpm

The observed trend of PM under EGR operation is similar to the one for CO. The quadratic increase of PM emission with increasing EGR is expected. The relative position of PM emissions at full load in respect with 75% load is as expected.

However, with the standard camshaft, PM emissions only start to increase at higher EGR%. The high boost and corresponding combustion pressures result in higher temperatures during the combustion, allowing for better soot oxidation. It is seen in Figure 10 that for the standard camshaft, the PM emission at full load is comparable to the PM at 75% load for measurements up to 15 EGR%. PM at full load exceeds PM at 75% load, contrary to expectations from literature. The main reason for this behavior can be found in the use of the turbine bypass. Boost pressure has to be limited to prevent excessive

combustion pressures. Comparable boost pressures over the entire EGR range are observed at 100% load and for EGR% up to 17 % at 75% load. This results in comparable soot oxidation. The boost pressures also result in combustion with higher temperatures and pressures when operating with the standard camshaft, explaining the lower PM emissions of this configuration.

5. Summary & recommendations

The effects of EGR operation on a modified ABC test engine were investigated. The use of a high-pressure cooled EGR loop gives a linear decrease in NO_x-emissions with increasing EGR%. Reductions of up to 70% of NO_x were attained at different loads. The greatest NO_x reduction could be achieved with Miller timing, due to expansion cooling.

However, the application of EGR has a significant influence on BSFC and the emissions of CO and PM. The emission of UHC is not negatively influenced by EGR application, contrary to the results of most studies performed on smaller engines. Operation with the standard camshaft offers possibilities for higher fuel economy. Under EGR operation, a certain BSFC corresponds to a lower NO_x level compared to using the Miller timing. Also, CO and PM emissions are much lower throughout the entire load region, due to higher volumetric efficiency.

Using the standard camshaft, an injection retardation could lower the NO_x emissions somewhat further. There will be a penalty for fuel consumption, but a relatively large buffer of BSFC compared to Miller operation is present. Also, retarding injection would lower combustion pressures, somewhat reducing the need for large amounts of turbine bypass with the wastegate.

The focus in this work was put on the high load effects of EGR, because of the high weighing factors of these load points in emission cycle calculations. However, EGR also presents difficulties under low load operation where CO and PM emissions are high. A technique to address the low load issues is using a common rail injection system. Higher available injection pressures, independent of load, and the use of a post-injection to address CO and PM emissions are then

possible. An injection advance during low load operation would raise combustion pressures and shorten combustion duration, lowering the emissions of CO and PM, while increasing efficiency.

In the current engine setup, the turbocharger is not suited for combination with the standard camshaft. Utilizing a Variable Geometry Turbine (VGT) or two-stage turbo-charging would enable a wider operating region.

A new accurate method was developed to measure EGR% based on the energy balance in the EGR cooler. A combined relative error of 2.2% is achieved. Previous methods were unreliable presumably because of bad mixing at the measurement location, or inaccurate operator actions. This method is fool-proof and uses simple sensors that do not require extensive maintenance.

From the results presented in this paper, it can be concluded that the EGR system is an essential part of an engine concept in order to fulfill IMO Tier III NO_x requirements. However, further investigation is needed to address its inherent drawbacks. The application of a common rail system will be the next important step in the optimization of this engine concept, together with careful matching of turbo-charging and the engine.

6. Acknowledgments

The investigations presented in this paper have been carried out with the financial support of Anglo Belgian Corporation (ABC), and the Institute for the Promotion of Innovation through Science and Technology in Flanders (IWT-Vlaanderen) research and development (IWT O&O 110579) in cooperation with ABC (CRISTAL-project). These financial supports are gratefully acknowledged.

Symbols and abbreviations

ABC	Anglo Belgian Corporation
AFR	Air to Fuel Ratio
(A)TDC	(After) Top Dead Center
AHRR	Apparent Heat Release Rate
(B)BDC	(Before) Bottom Dead Center
CA	Crank Angle
DMAF	Differential Mass Air Flow
EGR	Exhaust Gas Recirculation
EMP	Exhaust Manifold Pressure
EPA	US Environmental Protection Agency
HD	Heavy Duty
HR	Cumulative Heat Release
IMO	International Maritime Organization
IMP	Inlet Manifold Pressure
λ	Excess Air Factor
L_s	Stoichiometric air-to-fuel ratio
MFB	Mass Fraction burned
PM	Particulate Matter
SOI	Start of Injection
UHC	Unburned HydroCarbons

References

[1] B. Guan, R. Zhan, H. Lin, Z. Huang, Review of state of the art technologies of selective catalytic reduction of NOx from diesel engine exhaust, Applied Thermal Engineering 66 (2014) 395 – 414.

[2] M. Lamas, C. Rodriguez, Emissions from marine engines and NOx reduction methods, Journal of Maritime Research IX (2011) 77–82.

[3] Y. Wang, S. Zeng, J. Huang, Y. He, X. Huang, L. Lin, S. Li, Experimental investigation of applying Miller cycle to reduce NOx emission from diesel

engine, Proceedings of the Institution of Mechanical Engineers, Part A: Journal of Power and Energy 219 (8) (2005) 631–638.

[4] C. A. Rinaldini, E. Mattarelli, V. I. Golovitchev, Potential of the Miller cycle on a HSDI diesel automotive engine, Applied Energy 112 (2013) 102 – 119.

[5] J. Benajes, J. Serrano, S. Molina, R. Novella, Potential of Atkinson cycle combined with EGR for pollutant control in a HD diesel engine, Energy Conversion and Management 50 (2009) 174–183.

[6] J. Benajes, S. Molina, R. Novella, E. Belarte, Evaluation of massive exhaust gas recirculation and miller cycle strategies for mixing-controlled low temperature combustion in a heavy duty diesel engine, Energy (2014).

[7] F. Millo, M. G. Bernardi, Computational analysis of internal and external EGR strategies combined with Miller cycle concept for a two stage turbocharged medium speed marine diesel engine, SAE paper no. 2011-01-1142 (2011).

[8] B. Mohan, W. Yang, S. kiang Chou, Fuel injection strategies for performance improvement and emissions reduction in compression ignition engines - a review, Renewable and Sustainable Energy Reviews 28 (0) (2013) 664 – 676.

[9] International Maritime Organization, Revised MARPOL annex VI & NOx technical code 2008 - 2009 edition (2009).

[10] N. Xiros, Robust Control of Diesel Ship Propulsion, Advances in Industrial Control, Springer London, 2002.

[11] E. Knobbe, D. Stapersma, Some new ideas for performing heat release analysis, in: CIMAC 2001 Congress, Hamburg, 2001, pp. 654–664.

[12] D. Six, T. V. Herzele, L. Vervaeke, M. Bastiaen, J. Galle, S. Verhelst, Development and testing of an EGR system for medium speed diesel engines, SAE paper no. 2012-01-0680 (2012).

[13] M. Zheng, G. T. Reader, J. Hawley, Diesel engine exhaust gas recirculation - a review on advanced and novel concepts, Energy Conversion and Management 45 (6) (2004) 883 – 900.

[14] A. Maiboom, M. Tauzia, Xavier Tounsi, T. Jaine, Various effects of EGR on combustion and emissions on an automotive DI diesel engine : numerical and experimental study, SAE 2007-01-1834 (2007).

[15] R. Rogers, Engine Combustion: Pressure Measurement and Analysis, SAE International, Warrendale, PA, 2010, ISBN: 978-0-7680-1963-6.

[16] A. Maiboom, X. Tauzia, J.-F. Hetet, Experimental study of various effects of exhaust gas recirculation (EGR) on combustion and emissions of an automotive direct injection diesel engine, Energy 33 (1) (2008) 22 – 34.

[17] R. Schubiger, A. Bertola, K. Boulouchos, Influence of EGR on combustion and exhaust emissions of heavy duty DI-diesel engines equipped with common-rail injection systems, SAE paper no. 2001-01-3497 (2001).

[18] N. Ladommatos, S. M. Abdelhalim, H. Zhao, Z. Hu, Effects of EGR on heat release in diesel combustion, SAE paper no. 980184 (1998).

[19] G. Heider, P. Eilts, Improving the soot-NO_x-BSFC trade-off of medium speed 4-stroke diesel engine, in: CIMAC 2001 Congress, Hamburg, 2001, pp. 663–671.